UC Berkeley
UC Berkeley Previously Published Works

Title
Precision measurement of the Λc+ baryon mass

Permalink
https://escholarship.org/uc/item/95s0d52k

Journal
Physical Review D, 72(5)

ISSN
2470-0010

Authors
Aubert, B
Barate, R
Boutigny, D
et al.

Publication Date
2005-09-01

DOI
10.1103/physrevd.72.052006

Copyright Information
This work is made available under the terms of a Creative Commons Attribution License, availalbe at https://creativecommons.org/licenses/by/4.0/

Peer reviewed

eScholarship.org Powered by the California Digital Library
University of California

PHYSICAL REVIEW D **72,** 052006 (2005)

Precision measurement of the Λ_c^+ baryon mass

B. Aubert, R. Barate, D. Boutigny, F. Couderc, Y. Karyotakis, J. P. Lees, V. Poireau, V. Tisserand, and A. Zghiche
Laboratoire de Physique des Particules, F-74941 Annecy-le-Vieux, France

E. Grauges
IFAE, Universitat Autonoma de Barcelona, E-08193 Bellaterra, Barcelona, Spain

A. Palano, M. Pappagallo, and A. Pompili
Università di Bari, Dipartimento di Fisica and INFN, I-70126 Bari, Italy

J. C. Chen, N. D. Qi, G. Rong, P. Wang, and Y. S. Zhu
Institute of High Energy Physics, Beijing 100039, China

G. Eigen, I. Ofte, and B. Stugu
University of Bergen, Inst. of Physics, N-5007 Bergen, Norway

G. S. Abrams, M. Battaglia, A. B. Breon, D. N. Brown, J. Button-Shafer, R. N. Cahn, E. Charles, C. T. Day, M. S. Gill, A. V. Gritsan, Y. Groysman, R. G. Jacobsen, R. W. Kadel, J. Kadyk, L. T. Kerth, Yu. G. Kolomensky, G. Kukartsev, G. Lynch, L. M. Mir, P. J. Oddone, T. J. Orimoto, M. Pripstein, N. A. Roe, M. T. Ronan, and W. A. Wenzel
Lawrence Berkeley National Laboratory, Berkeley, California 94720, USA
and University of California, Berkeley, California 94720, USA

M. Barrett, K. E. Ford, T. J. Harrison, A. J. Hart, C. M. Hawkes, S. E. Morgan, and A. T. Watson
University of Birmingham, Birmingham, B15 2TT, United Kingdom

M. Fritsch, K. Goetzen, T. Held, H. Koch, B. Lewandowski, M. Pelizaeus, K. Peters, T. Schroeder, and M. Steinke
Ruhr Universität Bochum, Institut für Experimentalphysik 1, D-44780 Bochum, Germany

J. T. Boyd, J. P. Burke, N. Chevalier, and W. N. Cottingham
University of Bristol, Bristol BS8 1TL, United Kingdom

T. Cuhadar-Donszelmann, B. G. Fulsom, C. Hearty, N. S. Knecht, T. S. Mattison, and J. A. McKenna
University of British Columbia, Vancouver, British Columbia, Canada V6T 1Z1

A. Khan, P. Kyberd, M. Saleem, and L. Teodorescu
Brunel University, Uxbridge, Middlesex UB8 3PH, United Kingdom

A. E. Blinov, V. E. Blinov, A. D. Bukin, V. P. Druzhinin, V. B. Golubev, E. A. Kravchenko, A. P. Onuchin, S. I. Serednyakov, Yu. I. Skovpen, E. P. Solodov, and A. N. Yushkov
Budker Institute of Nuclear Physics, Novosibirsk 630090, Russia

D. Best, M. Bondioli, M. Bruinsma, M. Chao, S. Curry, I. Eschrich, D. Kirkby, A. J. Lankford, P. Lund, M. Mandelkern, R. K. Mommsen, W. Roethel, and D. P. Stoker
University of California at Irvine, Irvine, California 92697, USA

C. Buchanan, B. L. Hartfiel, and A. J. R. Weinstein
University of California at Los Angeles, Los Angeles, California 90024, USA

S. D. Foulkes, J. W. Gary, O. Long, B. C. Shen, K. Wang, and L. Zhang
University of California at Riverside, Riverside, California 92521, USA

D. del Re, H. K. Hadavand, E. J. Hill, D. B. MacFarlane, H. P. Paar, S. Rahatlou, and V. Sharma
University of California at San Diego, La Jolla, California 92093, USA

J. W. Berryhill, C. Campagnari, A. Cunha, B. Dahmes, T. M. Hong, M. A. Mazur, J. D. Richman, and W. Verkerke
University of California at Santa Barbara, Santa Barbara, California 93106, USA

 © 2005 The American Physical Society

T. W. Beck, A. M. Eisner, C. J. Flacco, C. A. Heusch, J. Kroseberg, W. S. Lockman, G. Nesom, T. Schalk, B. A. Schumm, A. Seiden, P. Spradlin, D. C. Williams, and M. G. Wilson
University of California at Santa Cruz, Institute for Particle Physics, Santa Cruz, California 95064, USA

J. Albert, E. Chen, G. P. Dubois-Felsmann, A. Dvoretskii, D. G. Hitlin, I. Narsky, T. Piatenko, F. C. Porter, A. Ryd, and A. Samuel
California Institute of Technology, Pasadena, California 91125, USA

R. Andreassen, S. Jayatilleke, G. Mancinelli, B. T. Meadows, and M. D. Sokoloff
University of Cincinnati, Cincinnati, Ohio 45221, USA

F. Blanc, P. Bloom, S. Chen, W. T. Ford, J. F. Hirschauer, A. Kreisel, U. Nauenberg, A. Olivas, P. Rankin, W. O. Ruddick, J. G. Smith, K. A. Ulmer, S. R. Wagner, and J. Zhang
University of Colorado, Boulder, Colorado 80309, USA

A. Chen, E. A. Eckhart, A. Soffer, W. H. Toki, R. J. Wilson, and Q. Zeng
Colorado State University, Fort Collins, Colorado 80523, USA

D. Altenburg, E. Feltresi, A. Hauke, and B. Spaan
Universität Dortmund, Institut fur Physik, D-44221 Dortmund, Germany

T. Brandt, J. Brose, M. Dickopp, V. Klose, H. M. Lacker, R. Nogowski, S. Otto, A. Petzold, G. Schott, J. Schubert, K. R. Schubert, R. Schwierz, and J. E. Sundermann
Technische Universität Dresden, Institut für Kern- und Teilchenphysik, D-01062 Dresden, Germany

D. Bernard, G. R. Bonneaud, P. Grenier, S. Schrenk, Ch. Thiebaux, G. Vasileiadis, and M. Verderi
Ecole Polytechnique, LLR, F-91128 Palaiseau, France

D. J. Bard, P. J. Clark, W. Gradl, F. Muheim, S. Playfer, and Y. Xie
University of Edinburgh, Edinburgh EH9 3JZ, United Kingdom

M. Andreotti, V. Azzolini, D. Bettoni, C. Bozzi, R. Calabrese, G. Cibinetto, E. Luppi, M. Negrini, and L. Piemontese
Università di Ferrara, Dipartimento di Fisica and INFN, I-44100 Ferrara, Italy

F. Anulli, R. Baldini-Ferroli, A. Calcaterra, R. de Sangro, G. Finocchiaro, P. Patteri, I. M. Peruzzi,* M. Piccolo, and A. Zallo
Laboratori Nazionali di Frascati dell'INFN, I-00044 Frascati, Italy

A. Buzzo, R. Capra, R. Contri, M. Lo Vetere, M. Macri, M. R. Monge, S. Passaggio, C. Patrignani, E. Robutti, A. Santroni, and S. Tosi
Università di Genova, Dipartimento di Fisica and INFN, I-16146 Genova, Italy

G. Brandenburg, K. S. Chaisanguanthum, M. Morii, E. Won, and J. Wu
Harvard University, Cambridge, Massachusetts 02138, USA

R. S. Dubitzky, U. Langenegger, J. Marks, S. Schenk, and U. Uwer
Universität Heidelberg, Physikalisches Institut, Philosophenweg 12, D-69120 Heidelberg, Germany

W. Bhimji, D. A. Bowerman, P. D. Dauncey, U. Egede, R. L. Flack, J. R. Gaillard, G. W. Morton, J. A. Nash, M. B. Nikolich, G. P. Taylor, and W. P. Vazquez
Imperial College London, London, SW7 2AZ, United Kingdom

M. J. Charles, W. F. Mader, U. Mallik, and A. K. Mohapatra
University of Iowa, Iowa City, Iowa 52242, USA

J. Cochran, H. B. Crawley, V. Eyges, W. T. Meyer, S. Prell, E. I. Rosenberg, A. E. Rubin, and J. Yi
Iowa State University, Ames, Iowa 50011-3160, USA

N. Arnaud, M. Davier, X. Giroux, G. Grosdidier, A. Höcker, F. Le Diberder, V. Lepeltier, A. M. Lutz, A. Oyanguren, T. C. Petersen, M. Pierini, S. Plaszczynski, S. Rodier, P. Roudeau, M. H. Schune, A. Stocchi, and G. Wormser
Laboratoire de l'Accélérateur Linéaire, F-91898 Orsay, France

C. H. Cheng, D. J. Lange, M. C. Simani, and D. M. Wright
Lawrence Livermore National Laboratory, Livermore, California 94550, USA

A. J. Bevan, C. A. Chavez, I. J. Forster, J. R. Fry, E. Gabathuler, R. Gamet, K. A. George, D. E. Hutchcroft, R. J. Parry, D. J. Payne, K. C. Schofield, and C. Touramanis
University of Liverpool, Liverpool L69 72E, United Kingdom

C. M. Cormack, F. Di Lodovico, W. Menges, and R. Sacco
Queen Mary, University of London, E1 4NS, United Kingdom

C. L. Brown, G. Cowan, H. U. Flaecher, M. G. Green, D. A. Hopkins, P. S. Jackson, T. R. McMahon, S. Ricciardi, and F. Salvatore
University of London, Royal Holloway and Bedford New College, Egham, Surrey TW20 0EX, United Kingdom

D. Brown and C. L. Davis
University of Louisville, Louisville, Kentucky 40292, USA

J. Allison, N. R. Barlow, R. J. Barlow, C. L. Edgar, M. C. Hodgkinson, M. P. Kelly, G. D. Lafferty, M. T. Naisbit, and J. C. Williams
University of Manchester, Manchester M13 9PL, United Kingdom

C. Chen, W. D. Hulsbergen, A. Jawahery, D. Kovalskyi, C. K. Lae, D. A. Roberts, and G. Simi
University of Maryland, College Park, Maryland 20742, USA

G. Blaylock, C. Dallapiccola, S. S. Hertzbach, R. Kofler, V. B. Koptchev, X. Li, T. B. Moore, S. Saremi, H. Staengle, and S. Willocq
University of Massachusetts, Amherst, Massachusetts 01003, USA

R. Cowan, K. Koeneke, G. Sciolla, S. J. Sekula, M. Spitznagel, F. Taylor, and R. K. Yamamoto
Massachusetts Institute of Technology, Laboratory for Nuclear Science, Cambridge, Massachusetts 02139, USA

H. Kim, P. M. Patel, and S. H. Robertson
McGill University, Montréal, Quebec, Canada H3A 2T8

A. Lazzaro, V. Lombardo, and F. Palombo
Università di Milano, Dipartimento di Fisica and INFN, I-20133 Milano, Italy

J. M. Bauer, L. Cremaldi, V. Eschenburg, R. Godang, R. Kroeger, J. Reidy, D. A. Sanders, D. J. Summers, and H. W. Zhao
University of Mississippi, University, Mississippi 38677, USA

S. Brunet, D. Côté, P. Taras, and B. Viaud
Université de Montréal, Laboratoire René J. A. Lévesque, Montréal, Quebec, Canada H3C 3J7

H. Nicholson
Mount Holyoke College, South Hadley, Massachusetts 01075, USA

N. Cavallo,[†] G. De Nardo, F. Fabozzi,[†] C. Gatto, L. Lista, D. Monorchio, P. Paolucci, D. Piccolo, and C. Sciacca
Università di Napoli Federico II, Dipartimento di Scienze Fisiche and INFN, I-80126, Napoli, Italy

M. Baak, H. Bulten, G. Raven, H. L. Snoek, and L. Wilden
NIKHEF, National Institute for Nuclear Physics and High Energy Physics, NL-1009 DB Amsterdam, The Netherlands

C. P. Jessop and J. M. LoSecco
University of Notre Dame, Notre Dame, Indiana 46556, USA

T. Allmendinger, G. Benelli, K. K. Gan, K. Honscheid, D. Hufnagel, P. D. Jackson, H. Kagan, R. Kass, T. Pulliam, A. M. Rahimi, R. Ter-Antonyan, and Q. K. Wong
Ohio State University, Columbus, Ohio 43210, USA

J. Brau, R. Frey, O. Igonkina, M. Lu, C. T. Potter, N. B. Sinev, D. Strom, J. Strube, and E. Torrence
University of Oregon, Eugene, Oregon 97403, USA

F. Galeazzi, M. Margoni, M. Morandin, M. Posocco, M. Rotondo, F. Simonetto, R. Stroili, and C. Voci
Università di Padova, Dipartimento di Fisica and INFN, I-35131 Padova, Italy

M. Benayoun, H. Briand, J. Chauveau, P. David, L. Del Buono, Ch. de la Vaissière, O. Hamon, M. J. J. John, Ph. Leruste, J. Malclès, J. Ocariz, L. Roos, and G. Therin
Universités Paris VI et VII, Laboratoire de Physique Nucléaire et de Hautes Energies, F-75252 Paris, France

P. K. Behera, L. Gladney, Q. H. Guo, and J. Panetta
University of Pennsylvania, Philadelphia, Pennsylvania 19104, USA

M. Biasini, R. Covarelli, S. Pacetti, and M. Pioppi
Università di Perugia, Dipartimento di Fisica and INFN, I-06100 Perugia, Italy

C. Angelini, G. Batignani, S. Bettarini, F. Bucci, G. Calderini, M. Carpinelli, R. Cenci, F. Forti, M. A. Giorgi, A. Lusiani, G. Marchiori, M. Morganti, N. Neri, E. Paoloni, M. Rama, G. Rizzo, and J. Walsh
Università di Pisa, Dipartimento di Fisica, Scuola Normale Superiore and INFN, I-56127 Pisa, Italy

M. Haire, D. Judd, and D. E. Wagoner
Prairie View A&M University, Prairie View, Texas 77446, USA

J. Biesiada, N. Danielson, P. Elmer, Y. P. Lau, C. Lu, J. Olsen, A. J. S. Smith, and A. V. Telnov
Princeton University, Princeton, New Jersey 08544, USA

F. Bellini, G. Cavoto, A. D'Orazio, E. Di Marco, R. Faccini, F. Ferrarotto, F. Ferroni, M. Gaspero, L. Li Gioi, M. A. Mazzoni, S. Morganti, G. Piredda, F. Polci, F. Safai Tehrani, and C. Voena
Università di Roma La Sapienza, Dipartimento di Fisica and INFN, I-00185 Roma, Italy

H. Schröder, G. Wagner, and R. Waldi
Universität Rostock, D-18051 Rostock, Germany

T. Adye, N. De Groot, B. Franek, G. P. Gopal, E. O. Olaiya, and F. F. Wilson
Rutherford Appleton Laboratory, Chilton, Didcot, Oxon, OX11 0QX, United Kingdom

R. Aleksan, S. Emery, A. Gaidot, S. F. Ganzhur, P.-F. Giraud, G. Graziani, G. Hamel de Monchenault, W. Kozanecki, M. Legendre, G. W. London, B. Mayer, G. Vasseur, Ch. Yèche, and M. Zito
DSM/Dapnia, CEA/Saclay, F-91191 Gif-sur-Yvette, France

M. V. Purohit, A. W. Weidemann, J. R. Wilson, and F. X. Yumiceva
University of South Carolina, Columbia, South Carolina 29208, USA

T. Abe, M. T. Allen, D. Aston, N. Bakel, R. Bartoldus, N. Berger, A. M. Boyarski, O. L. Buchmueller, R. Claus, J. P. Coleman, M. R. Convery, M. Cristinziani, J. C. Dingfelder, D. Dong, J. Dorfan, D. Dujmic, W. Dunwoodie, S. Fan, R. C. Field, T. Glanzman, S. J. Gowdy, T. Hadig, V. Halyo, C. Hast, T. Hryn'ova, W. R. Innes, M. H. Kelsey, P. Kim, M. L. Kocian, D. W. G. S. Leith, J. Libby, S. Luitz, V. Luth, H. L. Lynch, H. Marsiske, R. Messner, D. R. Muller, C. P. O'Grady, V. E. Ozcan, A. Perazzo, M. Perl, B. N. Ratcliff, A. Roodman, A. A. Salnikov, R. H. Schindler, J. Schwiening, A. Snyder, J. Stelzer, D. Su, M. K. Sullivan, K. Suzuki, S. Swain, J. M. Thompson, J. Va'vra, M. Weaver,

W. J. Wisniewski, M. Wittgen, D. H. Wright, A. K. Yarritu, K. Yi, and C. C. Young
Stanford Linear Accelerator Center, Stanford, California 94309, USA

P. R. Burchat, A. J. Edwards, S. A. Majewski, B. A. Petersen, and C. Roat
Stanford University, Stanford, California 94305-4060, USA

M. Ahmed, S. Ahmed, M. S. Alam, J. A. Ernst, M. A. Saeed, F. R. Wappler, and S. B. Zain
State University of New York, Albany, New York 12222, USA

W. Bugg, M. Krishnamurthy, and S. M. Spanier
University of Tennessee, Knoxville, Tennessee 37996, USA

R. Eckmann, J. L. Ritchie, A. Satpathy, and R. F. Schwitters
University of Texas at Austin, Austin, Texas 78712, USA

J. M. Izen, I. Kitayama, X. C. Lou, and S. Ye
University of Texas at Dallas, Richardson, Texas 75083, USA

F. Bianchi, M. Bona, F. Gallo, and D. Gamba
Università di Torino, Dipartimento di Fisica Sperimentale and INFN, I-10125 Torino, Italy

M. Bomben, L. Bosisio, C. Cartaro, F. Cossutti, G. Della Ricca, S. Dittongo, S. Grancagnolo, L. Lanceri, and L. Vitale
Università di Trieste, Dipartimento di Fisica and INFN, I-34127 Trieste, Italy

F. Martinez-Vidal
IFIC, Universitat de Valencia-CSIC, E-46071 Valencia, Spain

R. S. Panvini[‡]
Vanderbilt University, Nashville, Tennessee 37235, USA

Sw. Banerjee, B. Bhuyan, C. M. Brown, D. Fortin, K. Hamano, R. Kowalewski, J. M. Roney, and R. J. Sobie
University of Victoria, Victoria, British Columbia, Canada V8W 3P6

J. J. Back, P. F. Harrison, T. E. Latham, and G. B. Mohanty
Department of Physics, University of Warwick, Coventry CV4 7AL, United Kingdom

H. R. Band, X. Chen, B. Cheng, S. Dasu, M. Datta, A. M. Eichenbaum, K. T. Flood, M. Graham, J. J. Hollar, J. R. Johnson, P. E. Kutter, H. Li, R. Liu, B. Mellado, A. Mihalyi, Y. Pan, R. Prepost, P. Tan, J. H. von Wimmersperg-Toeller, S. L. Wu, and Z. Yu
University of Wisconsin, Madison, Wisconsin 53706, USA

H. Neal
Yale University, New Haven, Connecticut 06511, USA

(*BABAR* Collaboration)

(Received 1 July 2005; published 22 September 2005)

The Λ_c^+ baryon mass is measured using $\Lambda_c^+ \to \Lambda K_S^0 K^+$ and $\Lambda_c^+ \to \Sigma^0 K_S^0 K^+$ decays reconstructed in 232 fb^{-1} of data collected with the *BABAR* detector at the PEP-II asymmetric-energy e^+e^- storage ring. The Λ_c^+ mass is measured to be 2286.46 ± 0.14 MeV$/c^2$. The dominant systematic uncertainties arise from the amount of material in the tracking volume and from the magnetic field strength.

[*]Also with Università di Perugia, Dipartimento di Fisica, Perugia, Italy.

[†]Also with Università della Basilicata, Potenza, Italy.

[‡]Deceased.

DOI: 10.1103/PhysRevD.72.052006 PACS numbers: 14.20.Lq

I. INTRODUCTION

The invariant masses of the stable charmed hadrons are currently reported by the Particle Data Group (PDG) with a precision of about 0.5–0.6 MeV/c^2 [1]. The best individual measurements have a statistical and systematic precision of about 0.5 MeV/c^2 and use data samples of a few hundred events. The *BABAR* data contains large samples of many charmed-hadron decays and, due to the excellent momentum and vertex resolution in *BABAR*, many of the decay modes can be reconstructed with an event-by-event mass uncertainty of a few MeV/c^2. We can therefore significantly improve the precision on the charm-hadron mass measurements.

In this analysis we present a precision measurement of the Λ_c^+ mass. The measurement is based on the reconstruction of the decay modes $\Lambda_c^+ \to \Lambda K_S^0 K^+$ and $\Lambda_c^+ \to \Sigma^0 K_S^0 K^+$ [2]. Because almost all of the Λ_c^+ invariant mass in these decays results from the well-known rest-mass values of the Λ_c^+ decay products, the systematic uncertainty in the reconstructed mass is significantly reduced compared to the precision obtained in other decay modes. Large samples of $\Lambda_c^+ \to pK^-\pi^+$ and $\Lambda_c^+ \to pK_S^0$ decays are used for cross-checks and studies of systematic uncertainties.

II. ANALYSIS METHOD

The measurement of invariant mass relies on precise and unbiased measurements of particle three momenta. If the chosen decay mode contains any photons, unbiased energy and position measurements in the electromagnetic calorimeter (EMC) are also necessary. The momentum measurement depends on a well-aligned detector, precise knowledge of the magnetic field and material distribution in the tracking volume, and mass-dependent corrections for the energy loss of charged particles passing through the detector material. All three requirements are met to a large degree by the *BABAR* detector and its event reconstruction algorithms. We quantify residual systematic effects in studies of various control samples. To minimize such contributions to the systematic uncertainty, we choose to measure the Λ_c^+ mass by using decay modes with a low Q value, where the Q value for a decay $a \to b + c + \ldots$ is defined as

$$Q = m(a) - m(b) - m(c) - \ldots$$

Uncertainties related to track reconstruction, such as those involving energy-loss correction or magnetic field strength, tend to scale with the Q value.

The main signal mode used in this analysis is $\Lambda_c^+ \to \Lambda K_S^0 K^+$, which has a Q value of 177.9 MeV/c^2 calculated using the PDG Λ_c^+ mass. The branching ratio $\Gamma(\Lambda_c^+ \to \Lambda \overline{K}^0 K^+)/\Gamma(\Lambda_c^+ \to pK^-\pi^+)$ was measured by CLEO to be $0.12 \pm 0.02 \pm 0.02$ [3]. BELLE observed that about 25% of these decays proceed through $\Xi(1690)^0 K^+$ [4]. Since the $\Xi(1690)^0$ baryon has a width of several MeV/c^2 and its mass is not well known, it does not help in constraining the Λ_c^+ mass. We reconstruct the Λ and K_S^0 only in their charged decay modes, $\Lambda \to p\pi^-$ and $K_S^0 \to \pi^+\pi^-$, which account for about 44% of $\Lambda_c^+ \to \Lambda K_S^0 K^+$ decays. To obtain the most precise Λ_c^+ mass value, the long-lived particles are reconstructed with their mass values constrained to their respective PDG values.

A second low Q value Λ_c^+ decay mode, $\Lambda_c^+ \to \Sigma^0 K_S^0 K^+$, has been studied also. With the Q value of 100.9 MeV/c^2 it has the potential for an even lower systematic uncertainty. The results of this study indicate that the branching fraction for this decay mode is significantly smaller than for the $\Lambda_c^+ \to \Lambda K_S^0 K^+$ decay mode, which makes the statistical precision worse than the total precision of the $\Lambda_c^+ \to \Lambda K_S^0 K^+$ mode. The decay also requires the measurement of a photon from the $\Sigma^0 \to \Lambda\gamma$ decay and this introduces an additional systematic uncertainty.

For $\Lambda_c^+ \to \Lambda K_S^0 K^+$ decays, the event-by-event uncertainty on the invariant mass is about 2 MeV/c^2; hence, with a few thousand reconstructed signal events, the statistical uncertainty is below 50 keV/c^2 and the dominant uncertainty is systematic. The major part of the systematic uncertainty is estimated directly from the data by redoing the track fits with different assumptions on the amounts of detector material or the magnetic field strength and measuring how much the invariant-mass value changes with each assumption. The candidate selection criteria have been optimized on simulated events to minimize the expected systematic uncertainty.

To check that the procedure for estimating the systematic uncertainty is reasonable, we study large samples of Λ and K_S^0 decays. The goal is to ensure that the measured mass values are consistent with the PDG values within the systematic uncertainty we estimate using the same procedure as for the signal mode. Large samples of $\Lambda_c^+ \to pK^-\pi^+$ and $\Lambda_c^+ \to pK_S^0$ decays also are used and give invariant-mass measurements that are consistent with the signal when their larger systematic uncertainties are taken into account.

III. THE *BABAR* DETECTOR

The *BABAR* detector is described in detail elsewhere [5]. The momenta of charged particles are measured with a combination of a five-layer silicon vertex tracker (SVT) and a 40-layer drift chamber (DCH) in a 1.5-T solenoidal magnetic field. The momentum resolution is measured to be $\sigma(p_T)/p_T = 0.0013(p_T/\mathrm{GeV}/c) \oplus 0.0045$. A detector of internally reflected Cherenkov radiation (DIRC) is

used in charged particle identification. Kaons and protons are identified with likelihood ratios calculated from dE/dx measurements in the SVT and DCH, and from the observed pattern of Cherenkov light in the DIRC [6]. A finely segmented CsI(Tl) electromagnetic calorimeter is used to detect and measure photons and neutral hadrons, and to identify electrons. The instrumented flux return contains resistive plate chambers for muon and long-lived neutral-hadron identification. For event simulation we use the Monte Carlo generator EVTGEN [7] with a full detector simulation that uses GEANT4 [8].

The most critical component of this analysis is the quality of the track reconstruction. In order to maximize tracking efficiency, the track-finding algorithm is based on tracks found by the trigger system and by stand-alone track reconstruction in the SVT and in the DCH. Once a track has been found, the track parameters are determined using a Kalman filter algorithm [9], which makes optimal use of the hit information and corrects for energy loss and multiple scattering in the material traversed and for inhomogeneities in the magnetic field. The material-traversal corrections change the track momentum according to the expected average energy loss and increase the covariance for track parameters to account for both multiple scattering and the variance in the energy loss. The energy loss depends on the particle velocity, therefore each track fit is performed separately for five particle hypotheses: electron, muon, pion, kaon, and proton. A simplified model of the *BABAR* detector material distribution is used in the Kalman filter algorithm in order to maintain reasonable execution time. The main layers of material traversed by a particle originating from the interaction point are the beam pipe at a radius of 2.5 cm, consisting of about 1.4 mm of beryllium and 1.5 mm of cooling water; five layers of 300 μm-thick silicon detectors at radii from 3.3 to 15 cm; a 2-mm-thick carbon-fiber tube at a radius of 22 cm supporting the SVT and beam line magnets; and the inner wall of the DCH at a radius of 24 cm, which is a 1-mm-thick beryllium tube. Part of the support structure for the silicon detectors is modeled by increasing the thickness of each layer in the silicon detector by 60 μm, while the effect of the DCH gas is modeled as a series of discrete material contributions. Detailed knowledge of the magnetic field also is essential to the track reconstruction. This is discussed in Sec. VII B below.

IV. DATA SAMPLE

The data sample used for the Λ_c^+ mass measurement comprises an integrated luminosity of 232 fb^{-1} collected from e^+e^- collisions at or 40 MeV below the $\Upsilon(4S)$ resonance. For the studies of Λ and K_S^0 decays only a small subsample of the data is used due to the high production rates of these hadrons. Studies of simulated events are performed using Monte Carlo samples of generic $e^+e^- \to B\overline{B}$ and $e^+e^- \to q\bar{q}(q = u, d, s, c)$ continuum events with an integrated luminosity equivalent to 240 to 275 fb^{-1}. More than 230 000 simulated $\Lambda_c^+ \to \Lambda K_S^0 K^+$ decays and 60 000 simulated $\Lambda_c^+ \to \Sigma^0 K_S^0 K^+$ decays are used for studies of systematic uncertainty.

V. EVENT SELECTION

A. $\Lambda_c^+ \to \Lambda K_S^0 K^+$ selection

The $\Lambda_c^+ \to \Lambda K_S^0 K^+$ signal is reconstructed using only the charged two-body decay modes of the Λ and K_S^0 hadrons. We form Λ candidates from two tracks, one of which must be identified as a proton, and, after fitting to a common vertex, we require the combined invariant mass to be between 1106 and 1125 MeV/c^2. For surviving candidates, the two tracks are fit to a common vertex with the invariant mass constrained to the PDG Λ mass. The probability of this mass-constrained vertex fit is required to be above 10^{-3}. Similarly, a K_S^0 candidate is formed from two tracks, neither of which belongs to the Λ candidate, with a combined invariant mass between 460 and 530 MeV/c^2. For surviving K_S^0 candidates, the two daughter tracks are fit to a common vertex with the mass constrained to the PDG K_S^0 mass and the fit probability is required to be higher than 10^{-3}. The Λ and K_S^0 candidates are then combined with a fifth track, identified as a charged kaon, in a fit to a common vertex to form a Λ_c^+ candidate. The Λ_c^+ candidate must have an invariant mass between 2250 MeV/c^2 and 2330 MeV/c^2. The probability of the vertex fit should be greater than 10^{-3}. To suppress combinatorial background, the signed decay length of a K_S^0 candidate is required to be larger than 3 times its estimated uncertainty. The signed decay length is defined as the distance between the Λ_c^+ and K_S^0 candidate along the K_S^0 momentum in the center-of-mass (c.m.) frame. To further suppress background, which results mainly from B decays, the momentum (p^*) of the Λ_c^+ candidate in the e^+e^- c.m. is required to be at least 2 GeV/c. This requirement also helps to reduce systematic uncertainties that affect mainly low-momentum tracks. The selection efficiency, not including branching fractions, is about 15% for $\Lambda_c^+ \to \Lambda K_S^0 K^+$ decays with Λ_c^+ c.m. momentum larger than 2 GeV/c. The background is suppressed sufficiently to not be an issue for the Λ_c^+ mass measurement.

B. $\Lambda_c^+ \to \Sigma^0 K_S^0 K^+$ selection

The $\Lambda_c^+ \to \Sigma^0 K_S^0 K^+$ mode is reconstructed from $\Sigma^0 \to \Lambda\gamma$ and Λ and K_S^0 hadrons decaying into two charged particles. The Λ and K_S^0 candidates are formed in the same way as in the $\Lambda_c^+ \to \Lambda K_S^0 K^+$ selection. A Σ^0 candidate is formed by combining a Λ candidate with a photon and requiring the combined invariant mass to be between 1184 and 1196 MeV/c^2. A photon candidate is defined as an energy deposit in the EMC of at least 30 MeV that is not associated with any track and has a lateral moment [10] of its shower energy deposition of less than 0.8. If several

photons can be combined with a Λ to form Σ^0 candidates, only the candidate with the most energetic photon is retained in order to avoid double counting. The Σ^0 candidates are fit with their mass constrained to the PDG mass and are combined with K^0_S and K^+ candidates to form Λ^+_c candidates that must satisfy the same invariant mass, vertex probability, and p^* requirements as $\Lambda^+_c \to \Lambda K^0_S K^+$ candidates. The selection efficiency, not including branching fractions, is estimated to be about 8% for $\Lambda^+_c \to \Sigma^0 K^0_S K^+$ decays with Λ^+_c c.m. momentum larger than 2 GeV/c.

From simulation we expect that 18% of the $\Lambda^+_c \to \Sigma^0 K^0_S K^+$ decays are reconstructed with the wrong photon in the Σ^0 candidate. Because of the low energy of the photon and the mass constraint on the Σ^0 candidate, these Λ^+_c candidates still have the correct mass on average, but the mass resolution of these candidates is significantly degraded.

C. $\Lambda^+_c \to pK^-\pi^+$ selection

$\Lambda^+_c \to pK^-\pi^+$ candidates are formed from three tracks identified as a proton, a kaon, and a pion with a combined invariant mass between 2240 and 2330 MeV/c^2. The tracks are fit to a common vertex and the probability of the vertex fit is required to be greater than 10^{-3}. The signal-selection efficiency is about 42% and depends on the Λ^+_c momentum.

D. $\Lambda^+_c \to pK^0_S$ selection

For the $\Lambda^+_c \to pK^0_S$ decay mode, the K^0_S candidates are required to satisfy the same criteria as in the $\Lambda^+_c \to \Lambda K^0_S K^+$ mode, but with the further constraint that the decay angle θ of the π^+ in the K^0_S rest frame with respect to the K^0_S line-of-flight must satisfy $|\cos\theta| < 0.97$. This removes contamination from γ conversions. The K^0_S candidates are combined with tracks identified as protons in a fit to a common vertex and the resulting Λ^+_c candidates are required to have an invariant mass between 2240 and 2330 MeV/c^2. The probability of the vertex fit is required to be above 10^{-3}. The signal-selection efficiency is about 41% and depends on the Λ^+_c momentum.

E. $\Lambda \to p\pi^-$ and $K^0_S \to \pi^+\pi^-$ selection

For the cross-check studies in Sec. VII, large samples of Λ and K^0_S decays are reconstructed using similar criteria as those used to select Λ and K^0_S candidates for $\Lambda^+_c \to \Lambda K^0_S K^+$ decays. The mass-constrained vertex fits are replaced with geometric vertex fits with the requirement of a fit probability greater than 10^{-2}. For both Λ and K^0_S candidates the signed decay length calculated with respect to the e^+e^- interaction point is required to be larger than 3 times its uncertainty.

VI. SIGNAL FITS

The invariant-mass distribution for the $\Lambda^+_c \to \Lambda K^0_S K^+$ candidates is shown in Fig. 1. A clear Λ^+_c signal peak is observed. A binned maximum likelihood fit to the mass distribution is performed using a sum of two Gaussians with a common mean for the Λ^+_c signal function. The background is described by a linear function as suggested by simulation studies. The fit parameter values are given in Table I. Note that the uncertainty on the mean mass is statistical only and a correction for underestimated energy loss described in the next section has not been applied to the fitted mass.

The invariant-mass distribution for the $\Lambda^+_c \to \Sigma^0 K^0_S K^+$ candidates is shown in Fig. 2. A small but significant Λ^+_c signal peak is observed. The figure also shows the expected background under the Λ^+_c peak from $\Lambda^+_c \to \Sigma^0 K^0_S K^+$ decays with a correct Λ but a wrong photon used in candidate selection. A binned maximum likelihood fit of the mass distribution is performed using a single Gaussian for the Λ^+_c signal. The background is described by a linear function. The wrongly reconstructed $\Lambda^+_c \to \Sigma^0 K^0_S K^+$ can-

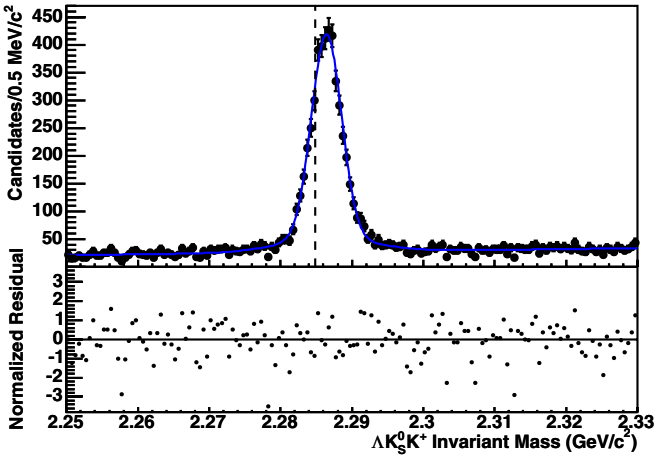

FIG. 1 (color online). Invariant-mass distribution for $\Lambda^+_c \to \Lambda K^0_S K^+$ candidates. The lower part of the figure shows the normalized fit residuals. The dashed line indicates the present PDG value.

TABLE I. Fit parameter values for the $\Lambda^+_c \to \Lambda K^0_S K^+$ and $\Lambda^+_c \to \Sigma^0 K^0_S K^+$ signals together with the HWHM calculated from these values. A correction to the mass values for underestimated energy loss has not been applied.

Parameter	$\Lambda^+_c \to \Lambda K^0_S K^+$	$\Lambda^+_c \to \Sigma^0 K^0_S K^+$
Fitted mass (MeV/c^2)	2286.44 ± 0.04	2286.29 ± 0.18
Signal yield (events)	4627 ± 84	264 ± 20
Narrow width (MeV/c^2)	2.08 ± 0.07	2.04 ± 0.18
Broad width (MeV/c^2)	6.39 ± 1.22	···
Narrow fraction	(83 ± 3)%	···
HWHM (MeV/c^2)	2.55 ± 0.06	2.41 ± 0.22

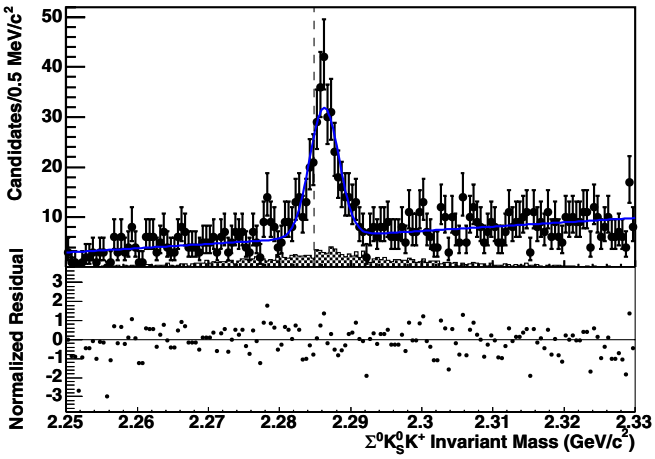

FIG. 2 (color online). Invariant mass of reconstructed $\Lambda_c^+ \to \Sigma^0 K_S^0 K^+$ candidates. The hashed histogram is the expected contribution from signal events with a wrongly assigned photon. The lower part of the figure shows the normalized fit residuals. The dashed line indicates the present PDG value.

didates are absorbed into the signal and background because they peak at the Λ_c^+ mass. The fit parameter values are given in Table I.

The invariant-mass distributions for the four control modes are shown in Fig. 3. The Λ and K_S^0 signals are fit to a sum of three Gaussians with common mean, while the two Λ_c^+ signals are fit to a sum of two Gaussians with common mean. The background in all four cases is modeled with a second-degree polynomial. The fit yields, mass, and signal half-width at half-maximum (HWHM) values are listed in Table II. The fitted mass values for the Λ and K_S^0 are significantly below the PDG values. This is due mainly to an underestimation of the energy loss in the detector material and is described in more detail in the next section.

VII. CROSS-CHECKS

The four control mode samples discussed above are used to understand the accuracy to which particle masses can be measured in *BABAR*.

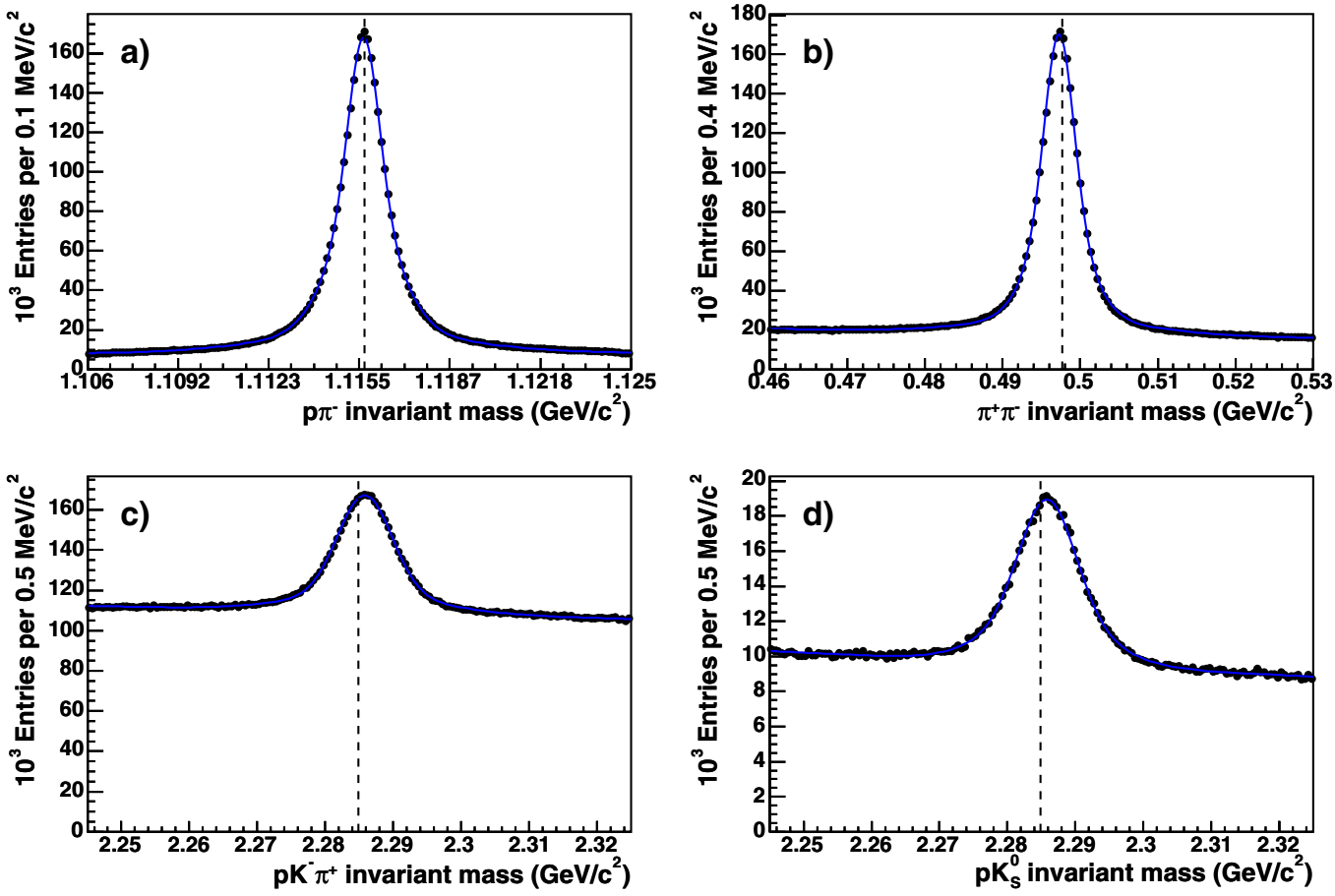

FIG. 3 (color online). Invariant-mass distribution of candidates used in cross-checks of systematic uncertainty. (a) $\Lambda \to p\pi^-$ decays. (b) $K_S^0 \to \pi^+\pi^-$ decays. (c) $\Lambda_c^+ \to pK^-\pi^+$ decays. (d) $\Lambda_c^+ \to pK_S^0$ decays. The dashed lines show the PDG mass values for these hadrons. A correction to the mass distributions for underestimated energy loss has not been applied.

TABLE II. Fit parameter values and calculated HWHM for the four decay modes used for cross-checks. A correction to each mass value for underestimated energy loss has not been applied.

Parameter	$\Lambda \to p\pi^-$	$K^0_S \to \pi^+\pi^-$	$\Lambda_c^+ \to pK^-\pi^+$	$\Lambda_c^+ \to pK^0_S$
PDG mass (MeV/c^2)	1115.683 ± 0.006	497.648 ± 0.022	2284.900 ± 0.600	2284.900 ± 0.600
Fitted mass (MeV/c^2)	1115.660 ± 0.001	497.305 ± 0.002	2285.845 ± 0.013	2285.876 ± 0.023
Signal yield (events)	3 192 700 ± 5800	2 463 900 ± 4900	1 449 300 ± 300	243 700 ± 900
HWHM (MeV/c^2)	0.853 ± 0.002	2.715 ± 0.005	5.147 ± 0.014	5.613 ± .046

A. Material dependence

The main systematic uncertainty on the Λ_c^+ mass comes from uncertainties in the energy-loss correction in charged particle tracking. The low Λ and K^0_S fitted mass values given in Table II indicate that the energy-loss correction may be underestimated. The long lifetimes of Λ and K^0_S hadrons enable us to study this in more detail. Figure 4 shows the Λ and K^0_S fitted mass values as a function of the radial distance from the interaction point to their decay point. The further the decay point is from the interaction point, the less material the charged daughter particles traverse, and so energy-loss corrections become less significant. The deviation from the PDG value is seen to be largest for decays closest to the interaction point, thereby strongly indicating that the underestimation of the mass values is due to insufficient material corrections. The lower fitted mass values at radii of 12 cm, 21 cm, and 23 cm coincide with vertices reconstructed inside or very near material sites. The same effect is observed in the reconstruction of simulated data. This is related to details of the incorporation of energy-loss corrections into the track-fit procedure in such circumstances.

The effect of increasing the amount of material assumed during the track reconstruction has been studied using several different scenarios. Figure 4 shows what happens if the material density in all parts of the SVT is increased uniformly by 20%. This is a gross simplification; however it removes most of the dependence on decay radius and moves the fitted hadron masses closer to their PDG values. The K^0_S mass is, however, still consistently low compared to the PDG value by about 0.15 MeV/c^2.

Another way to investigate the energy-loss correction is to study the fitted mass as a function of particle momentum. The lower the momentum of a charged particle, the more significant the energy-loss corrections become. Candidates are reconstructed from multiple tracks, but to simplify this investigation, the mass value is studied as a function of net candidate momentum calculated in the laboratory frame. Figure 5 shows the fitted mass value for $\Lambda_c^+ \to pK^-\pi^+$ and $\Lambda_c^+ \to pK^0_S$ candidates as a function of the laboratory momentum. Above 3 GeV/c the fitted mass value reaches a limit that is significantly above the PDG, while below 3 GeV/c it falls by more than 800 keV/c^2 as the momentum decreases. Similar behavior is observed for Λ and K^0_S hadrons, but the limiting value is reached at about 2 GeV/c. The decrease in mass is only about 60 keV/c^2 for Λ baryons and about 500 keV/c^2 for K^0_S mesons.

A similar effect is seen in a study of the reconstructed Λ, K^0_S, and Λ_c^+ mass as a function of their polar angle in the laboratory frame. The reconstructed mass is observed to be lower for particles at low angles where their decay products

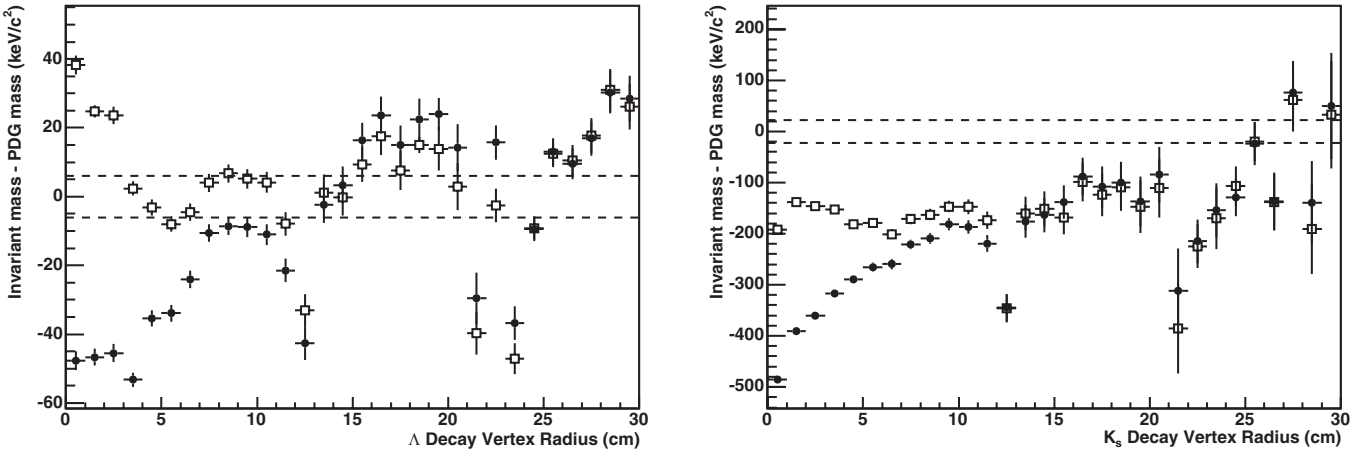

FIG. 4. Fitted mass values for $\Lambda \to p\pi^-$ (left) and $K^0_S \to \pi^+\pi^-$ (right) candidates minus the PDG value as a function of decay vertex radius. The solid circles are for track reconstruction with the normal amount of detector material. The open squares are for track reconstruction assuming 20% more material in the SVT. The dashed lines show the $\pm 1\sigma$ uncertainty on the PDG value for the masses.

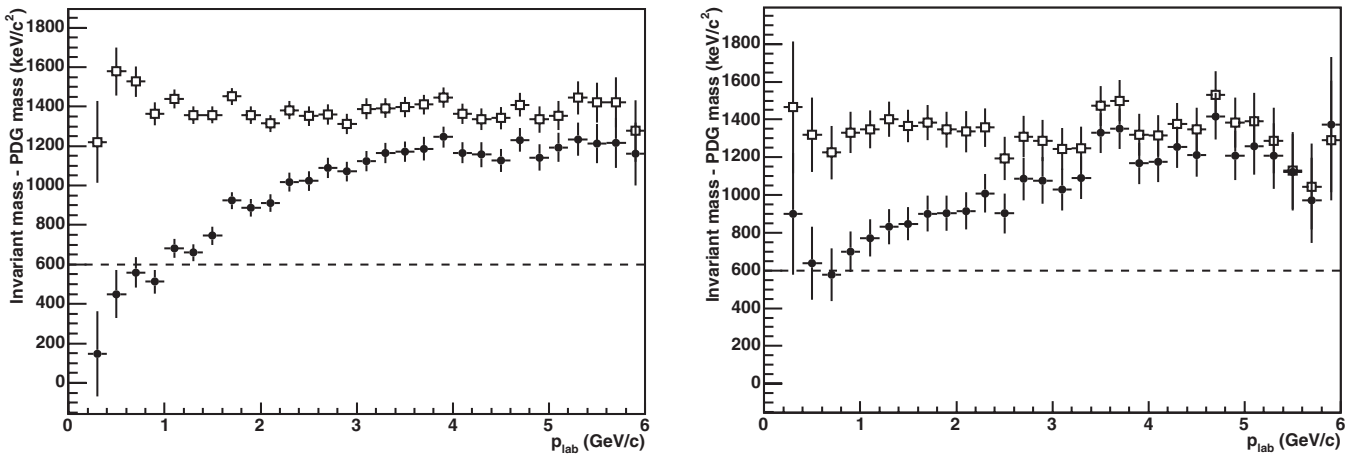

FIG. 5. Fitted mass value for $\Lambda_c^+ \to pK^-\pi^+$ (left) and $\Lambda_c^+ \to pK_S^0$ (right) candidates minus the PDG value as a function of Λ_c^+ laboratory momentum. The solid circles are for track reconstruction with the normal amount of detector material. The open squares are for track reconstruction assuming 20% more material in the SVT. The dashed line shows the $+1\sigma$ uncertainty on the PDG value of the Λ_c^+ mass.

on average traverse more material. Increasing the material density in the SVT by 20% also removes this angle dependence.

Increasing the assumed material density in the SVT by 20% is seen to greatly reduce the radial mass dependence in the Λ and K_S^0 control samples and the momentum and polar angle dependence in all control samples. We therefore apply this change to the reconstruction of the two low Q-value modes in order to obtain a more accurate mass measurement. However, since the K_S^0 mass still is not in agreement with the PDG value, we will use the largest observed variation in the fitted mass when we vary the material model as an estimate of the systematic uncertainty.

B. Magnetic field dependence

The momentum measurements, and thus the mass measurements, depend critically on the magnetic field. The main component of the magnetic field is the solenoid field, which has an average value of 1.5 T parallel to the beam axis. The field was mapped very precisely with movable Hall probes before the detector was installed; an NMR probe measured the absolute field strength. The field strength in the tracking volume is estimated to be known to an accuracy of about 0.2 mT. The second most significant field component comes from the permanent magnets used for the final focusing and bending of the beams. The magnet closest to the interaction point is about 20 cm away. The fringe fields in the tracking volume from the magnets are weak and have been measured. More uncertain is the contribution to the magnetization of the permanent magnet material due to the solenoid field. This effect is measured only at a few specific points with Hall and NMR probes, and we therefore rely on a finite element calculation to estimate the magnetization effect elsewhere. This model depends on the permeability of the magnets. These magnets are made of a SmCo alloy, which has a measured permeability $\mu = 1.07$ in the direction transverse to the solenoidal field. However this is an average over many samples, which range from 1.04 to 1.10. Furthermore in the direction of the solenoidal field the permeability of the SmCo elements is measured to be about 5% larger. Therefore, there is a significant uncertainty on this component of the field. The longitudinal field component at the interaction point from these magnets is about +9 mT. This increases the curvature of charged particle trajectories.

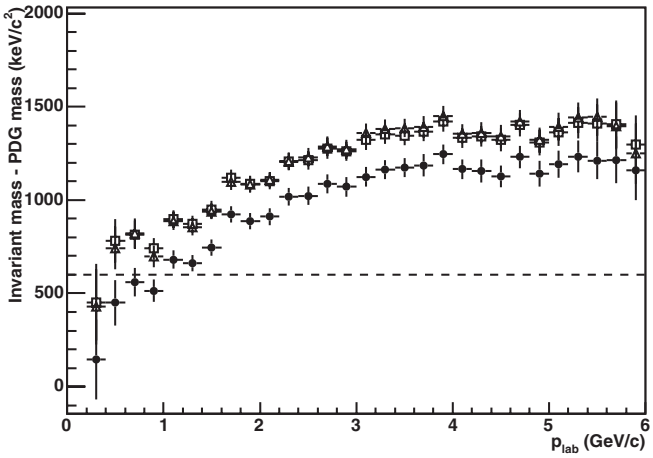

FIG. 6. Fitted mass of $\Lambda_c^+ \to pK^-\pi^+$ candidates minus the PDG value as a function of Λ_c^+ laboratory momentum. The additional energy-loss correction has not been applied. The solid circles are for track reconstruction with the normal magnetic field. The open squares are for track reconstruction assuming a 0.02% higher solenoid field. The open triangles are for track reconstruction assuming 20% higher magnetization. The dashed line shows the $+1\sigma$ uncertainty on the PDG value of the Λ_c^+ mass.

We vary the assumed solenoid field strength by 0.02% for the systematic uncertainty studies. The magnetization field is varied by 20% in order to account for differences between the direct field measurements and the permeability measurements. Figure 6 shows the effect on the fitted $\Lambda_c^+ \to pK^-\pi^+$ mass value as a function of momentum. The fitted mass value is seen to be shifted by the same amount independent of the momentum. The same is true for the other control samples, in particular, for the Λ and K_S^0 mass dependence on decay vertex radius. The control samples therefore provide little guidance on the magnetic field uncertainty.

C. ϕ dependence

Studies of the control samples reveal a significant dependence of the fitted mass value on the azimuthal angle ϕ of the hadron candidate momentum at the origin. This effect is not seen in simulated events. The ϕ dependence is shown in Fig. 7 for the K_S^0 and $\Lambda_c^+ \to pK^-\pi^+$ samples. The effect is seen to be roughly antisymmetric in ϕ with the lowest fitted mass at $\phi = \frac{\pi}{2}$, corresponding to upward going hadrons, and the largest fitted mass at $\phi = \frac{3\pi}{2}$, corresponding to downward going hadrons.

We have not been able to identify the source of the ϕ dependence, but we can estimate the potential impact on the Λ_c^+ mass measurement. The magnitude of the ϕ variation increases with the momentum of the reconstructed hadron. This shows that the variation is not due to some asymmetry in the material distribution that was unaccounted for in reconstruction, which would influence low-momentum particles the most. The ϕ dependence also is observed when only the DCH is used for reconstructing the tracks. This indicates that the source may be related to the internal alignment of the DCH, which is based on end-plate surveys done during construction of the chamber.

The ϕ dependence in the fitted mass can be reproduced qualitatively in simulated events by introducing an explicit ϕ dependence in the measured track momenta. To get the largest ϕ dependence at high momentum, the change has to be introduced as a bias in the track sagitta measurements. To a good approximation this corresponds to changing the transverse track momentum p_T according to

$$\frac{1}{p_T'} = \frac{1}{p_T} + \delta \sin\phi. \tag{1}$$

The constant δ is chosen to reproduce the observed magnitude of the ϕ dependence. The chosen value corresponds to a change in track sagitta of 11 μm, where the full sagitta for a track with 1 GeV/c transverse momentum is about 3 cm. Applying this modification to the $\Lambda_c^+ \to \Lambda K_S^0 K^+$ and $\Lambda_c^+ \to \Sigma^0 K_S^0 K^+$ Monte Carlo samples introduces a ϕ dependence in the fitted mass values with an amplitude of 55 keV/c^2 and 30 keV/c^2, respectively. When averaging over all ϕ, the fitted mass value does not change, but given that the source of the ϕ dependence is not understood, we use these amplitudes as estimates of systematic uncertainty.

VIII. SYSTEMATIC UNCERTAINTIES

The major sources of systematic uncertainty (energy-loss correction, magnetic field, and ϕ dependence) have been described in detail in the previous section. All of the known systematic uncertainties are listed in Table III. For the systematic uncertainty on the energy-loss correction we use the observed change in mass when the material density is increased uniformly by 10% in the tracking volume, which is a slightly larger change than the one from increasing the density in the SVT by 20%. The fit-procedure uncertainty summarizes the variation in the fitted mass value when the shapes of the signal, the background, and the choice of binning are varied. Imperfections and pos-

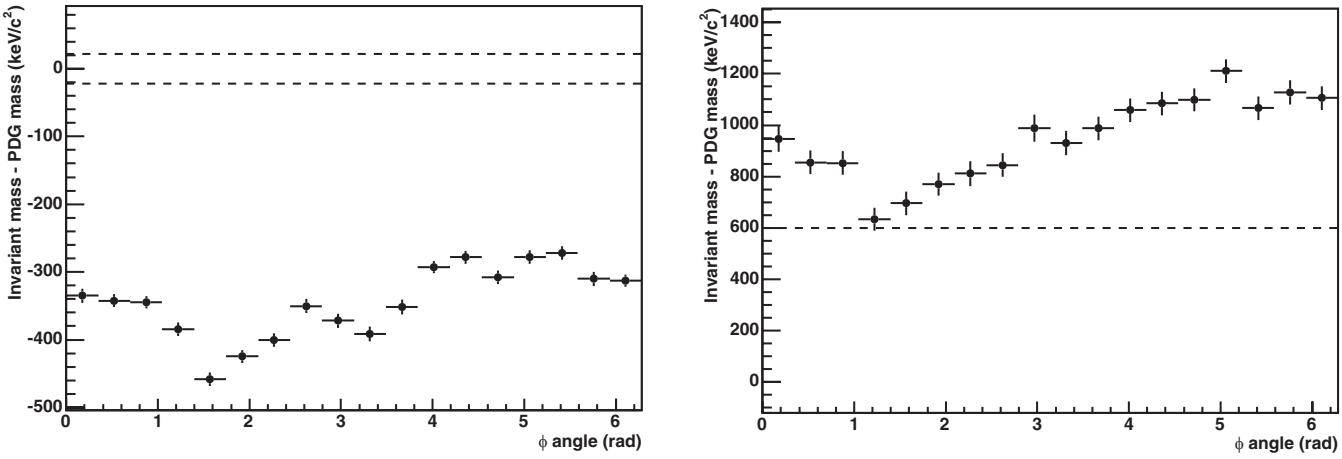

FIG. 7. Fitted mass value of $K_S^0 \to \pi^+\pi^-$ (left) and $\Lambda_c^+ \to pK^-\pi^+$ (right) candidates minus the PDG value as a function of the azimuthal direction. The additional energy-loss correction has not been applied. The dashed lines show the $\pm 1\sigma$ uncertainty on the PDG value of the masses.

TABLE III. Systematic uncertainty contributions to the Λ_c^+ mass measurements from the $\Lambda_c^+ \to \Lambda K_S^0 K^+$ and $\Lambda_c^+ \to \Sigma^0 K_S^0 K^+$ samples (in keV/c^2).

	$\Lambda_c^+ \to \Lambda K_S^0 K^+$	$\Lambda_c^+ \to \Sigma^0 K_S^0 K^+$
Solenoid field	± 60	± 30
Magnetization	± 68	± 29
Energy-loss correction	± 83	± 50
ϕ dependence	± 55	± 30
Fit procedure	± 38	± 71
SVT alignment	± 23	± 13
EMC energy scale	$\cdots$	± 46
Particle masses	± 27	± 58
Total systematic	± 144	± 126

sible biases in the procedure for the internal alignment of the SVT have been studied using simulated data samples, colliding beam dimuon data, and cosmic rays. The observed effects are modeled as internal SVT misalignments in signal events, which are then used to estimate the corresponding systematic uncertainty on the measured Λ_c^+ mass. For the $\Lambda_c^+ \to \Sigma^0 K_S^0 K^+$ mode, we vary the EMC energy scale by 5%, but due to the low energy of the photon and the mass constraint on the Σ^0, this has little effect on the fitted mass. Finally the Λ, K^+, and K_S^0 masses have uncertainties of 6, 16, and 22 keV/c^2 and the effect of these uncertainties on the Λ_c^+ mass has been estimated.

A. Energy-loss correction

The fitted Λ_c^+ mass values from Sec. VI need to be corrected for the underestimated energy loss. The correction is calculated by increasing the material density of the SVT by 20%, which is seen in the control samples to remove most of the momentum and decay-radius dependence. The corrections are 61 keV/c^2 and 18 keV/c^2 for the $\Lambda_c^+ \to \Lambda K_S^0 K^+$ and $\Lambda_c^+ \to \Sigma^0 K_S^0 K^+$ samples, respectively. This gives the following results for the Λ_c^+ mass:

$$m(\Lambda_c^+)_{\Lambda K_S^0 K^+} = 2286.501 \pm 0.042(\text{stat}) \pm 0.144(\text{syst})\ \text{MeV}/c^2,$$

$$m(\Lambda_c^+)_{\Sigma^0 K_S^0 K^+} = 2286.303 \pm 0.181(\text{stat}) \pm 0.126(\text{syst})\ \text{MeV}/c^2.$$

B. Combined result

The systematic uncertainties on the two measurements are highly, but not fully, correlated. We combine the two mass measurements using the best linear unbiased estimate technique [11]. Besides the statistical uncertainty, we consider the fit-procedure uncertainty and uncertainties related only to the $\Lambda_c^+ \to \Sigma^0 K_S^0 K^+$ mode to be uncorrelated, while the remaining systematic uncertainties are 100% correlated. The correlation coefficient for the two measurements is estimated to be 0.355. The combined mass result is

$$m(\Lambda_c^+) = 2286.46 \pm 0.14\ \text{MeV}/c^2.$$

C. Mass cross-checks

From the two large-Q-value Λ_c^+ data samples, we obtain measurements of the Λ_c^+ mass that can be compared to our more precise measurements from the $\Lambda_c^+ \to \Lambda K_S^0 K^+$ and $\Lambda_c^+ \to \Sigma^0 K_S^0 K^+$ samples. To keep the systematic uncertainty low, we use only $\Lambda_c^+ \to p K^- \pi^+$ and $\Lambda_c^+ \to p K_S^0$ candidates with laboratory momentum above 3 GeV/c, as Fig. 5 shows that those candidates have less dependence on the assumed amount of detector material. The resulting mass value for each decay mode from fitting the invariant-mass spectra with the sum of two Gaussian distributions with common mean is given in Table IV. The central values are corrected for the shift in mass observed when the material density of the SVT is increased by 20%. These corrections are 211 keV/c^2 and 145 keV/c^2 for the $\Lambda_c^+ \to p K^- \pi^+$ and $\Lambda_c^+ \to p K_S^0$ modes, respectively.

Table IV also lists the major systematic uncertainties. The solenoid and magnetization fields are varied as for the low-Q-value modes. For the energy-loss correction, we compare the effect of increasing the density of the SVT by 20% to the effect of increasing the density of material in the tracking volume by 10%, taking the larger change from the standard reconstruction as an estimate of the uncertainty. For both decays the larger effect is the 10% material change in the full tracking volume. The ϕ dependence is estimated by introducing a ϕ dependence in the simulation as described by Eq. (1). The uncertainty is the maximum change in mass introduced. The results

$$m(\Lambda_c^+)_{pK^-\pi^+} = 2286.39 \pm 0.02(\text{stat}) \pm 0.45(\text{syst})\ \text{MeV}/c^2,$$

$$m(\Lambda_c^+)_{pK_S^0} = 2286.36 \pm 0.03(\text{stat}) \pm 0.43(\text{syst})\ \text{MeV}/c^2,$$

TABLE IV. Fitted Λ_c^+ mass values and major contributions to the systematic uncertainty for the $\Lambda_c^+ \to p K^- \pi^+$ and $\Lambda_c^+ \to p K_S^0$ samples used for cross-checks (in MeV/c^2).

	$\Lambda_c^+ \to p K^- \pi^+$	$\Lambda_c^+ \to p K_S^0$
Fitted Mass	2286.182 ± 0.018	2286.216 ± 0.034
Corrected Mass	2286.393 ± 0.018	2286.361 ± 0.034
Solenoid field	± 0.181	± 0.196
Magnetization	± 0.207	± 0.222
Energy-loss correction	± 0.278	± 0.199
ϕ dependence	± 0.217	± 0.236
Total systematics	± 0.447	± 0.428

TABLE V. Fitted Λ and K_S^0 masses and the major contributions to the systematic uncertainty for candidates from the $\Lambda_c^+ \to \Lambda K_S^0 K^+$ sample (in MeV/c^2).

	Λ	K_S^0
Fitted Mass	1115.657 ± 0.014	497.359 ± 0.040
Corrected Mass	1115.679 ± 0.014	497.560 ± 0.040
Solenoid field	± 0.009	± 0.068
Magnetization	± 0.005	± 0.054
Energy-loss correction	± 0.040	± 0.242
ϕ dependence	± 0.006	± 0.059
Total systematic	± 0.041	± 0.264

are in good agreement with our main result but have larger systematic uncertainties.

The $\Lambda_c^+ \to \Lambda K_S^0 K^+$ sample is sufficiently large that we can fit the Λ and K_S^0 mass distributions for candidates that are combined to form the $\Lambda_c^+ \to \Lambda K_S^0 K^+$. In order to fit the Λ and K_S^0 mass distributions, the mass constraint is removed from the candidate reconstruction and the resulting invariant-mass spectra are fit with a double-Gaussian signal shape and a linear background. The resulting mass values and systematic uncertainties are listed in Table V. The mass correction for the underestimated energy loss and the systematic uncertainties are estimated as for the $\Lambda_c^+ \to pK^-\pi^+$ and $\Lambda_c^+ \to pK_S^0$ samples. The final results after the energy-loss correction,

$$m(\Lambda) = 1115.68 \pm 0.01(\text{stat}) \pm 0.04(\text{syst}) \text{ MeV}/c^2,$$

$$m(K_S^0) = 497.56 \pm 0.04(\text{stat}) \pm 0.26(\text{syst}) \text{ MeV}/c^2,$$

are in agreement with the PDG

$$m_{\text{PDG}}(\Lambda) = 1115.683 \pm 0.006 \text{ MeV}/c^2,$$

$$m_{\text{PDG}}(K_S^0) = 497.648 \pm 0.022 \text{ MeV}/c^2.$$

Since the Λ and K_S^0 candidates are the same candidates used in the final Λ_c^+ sample, the agreement with the PDG mass values gives further confidence in the Λ_c^+ mass result.

IX. SUMMARY

We have presented a precision measurement of the Λ_c^+ mass using the low-Q-value decay modes $\Lambda_c^+ \to \Lambda K_S^0 K^+$ and $\Lambda_c^+ \to \Sigma^0 K_S^0 K^+$ in order to minimize systematic uncertainty. The measured mass in the two modes is

$$m(\Lambda_c^+)_{\Lambda K_S^0 K^+} = 2286.501 \pm 0.042(\text{stat}) \pm 0.144(\text{syst}) \text{ MeV}/c^2,$$

$$m(\Lambda_c^+)_{\Sigma^0 K_S^0 K^+} = 2286.303 \pm 0.181(\text{stat}) \pm 0.126(\text{syst}) \text{ MeV}/c^2.$$

Combining these measurements, taking the correlated systematics into account, the final result for the Λ_c^+ mass is

$$m(\Lambda_c^+) = 2286.46 \pm 0.14 \text{ MeV}/c^2.$$

This result is in agreement with the mass values measured in other Λ_c^+ decay modes, although those are subject to large systematic uncertainty. The systematic uncertainty has been cross-checked using large data samples of Λ, K_S^0, and Λ_c^+ decays. The studies have shown that there is an underestimation of the energy-loss correction and a dependence on azimuthal angle in the standard *BABAR* track reconstruction. The impact on the mass measurement has been taken into account in the corresponding estimates of systematic uncertainty.

This Λ_c^+ mass measurement is the most precise measurement of an open charm-hadron mass to date and is an improvement in precision by more than a factor of 4 over the current PDG value of 2284.9 ± 0.6 MeV/c^2. Our result is about 2.5σ higher than the PDG value, which is based on several high Q-value decay modes, mainly $\Lambda_c^+ \to pK^-\pi^+$ decays. Theoretical calculations of the Λ_c^+ mass, such as those based upon lattice QCD [12] or advanced potential models [13], currently have significantly larger uncertainty than the experimental result presented here.

ACKNOWLEDGMENTS

We are grateful for the extraordinary contributions of our PEP-II colleagues in achieving the excellent luminosity and machine conditions that have made this work possible. The success of this project also relies critically on the expertise and dedication of the computing organizations that support *BABAR*. The collaborating institutions wish to thank SLAC for its support and the kind hospitality extended to them. This work is supported by the U.S. Department of Energy and National Science Foundation, the Natural Sciences and Engineering Research Council (Canada), Institute of High Energy Physics (China), the Commissariat à l'Energie Atomique and Institut National de Physique Nucléaire et de Physique des Particules (France), the Bundesministerium für Bildung und Forschung and Deutsche Forschungsgemeinschaft (Germany), the Istituto Nazionale di Fisica Nucleare (Italy), the Foundation for Fundamental Research on Matter (The Netherlands), the Research Council of Norway, the Ministry of Science and Technology of the Russian Federation, and the Particle Physics and Astronomy Research Council (United Kingdom). Individuals have received support from CONACyT (Mexico), the A. P. Sloan Foundation, the Research Corporation, and the Alexander von Humboldt Foundation.

[1] S. Eidelman *et al.*, Phys. Lett. B **592**, 1 (2004). We refer to averages or fits from this reference as ''PDG'' values.
[2] Throughout this paper, flavor-eigenstate decay modes imply also their charge conjugate.
[3] R. Ammar *et al.* (CLEO Collaboration), Phys. Rev. Lett. **74**, 3534 (1995).
[4] K. Abe *et al.* (Belle Collaboration), Phys. Lett. B **524**, 33 (2002).
[5] B. Aubert *et al.* (*BABAR* Collaboration), Nucl. Instrum. Methods Phys. Res., Sect. A **479**, 1 (2002).
[6] I. Adam *et al.* (*BABAR*-DIRC Collaboration), Nucl. Instrum. Methods Phys. Res., Sect. A **538**, 281 (2005).
[7] D. J. Lange, Nucl. Instrum. Methods Phys. Res., Sect. A **462**, 152 (2001).
[8] S. Agostinelli *et al.* (GEANT4 Collaboration), Nucl. Instrum. Methods Phys. Res., Sect. A **506**, 250 (2003).
[9] D. Brown, E. Charles, and D. Roberts, ''*The BABAR Track Fitting Algorithm*,'' Report No. CHEP 2000.
[10] A. Drescher *et al.* (ARGUS Collaboration), Nucl. Instrum. Methods Phys. Res., Sect. A **237**, 464 (1985).
[11] L. Lyons, D. Gibaut, and P. Clifford, Nucl. Instrum. Methods Phys. Res., Sect. A **270**, 110 (1988).
[12] K. C. Bowler *et al.* (UKQCD Collaboration), Phys. Rev. D **54**, 3619 (1996).
[13] C. Albertus, J. E. Amaro, E. Hernandez, and J. Nieves, Nucl. Phys. **A740**, 333 (2004).